# Surface Energy Balance Observations during MATERHORN

Sebastian W. Hoch[(1)], Derek Jensen[(1)], Jeffrey D. Massey, Eric R. Pardyjak[(1)], C. David Whiteman[(1)], Harindra J. Fernando[(2)]

[(1)]University of Utah, [(2)]University of Notre Dame

AMS 16TH Mountain Meteorology Conference
San Diego, CA, 18-22 August 2014

## (1) INTRODUCTION

The partitioning of the available energy at the Earth's surface varies widely by geographic location, land surface type, exposure, soil properties, and available moisture. The surface energy balance ultimately controls boundary layer development and evolution. Spatial energy balance differences lead to the formation of thermally driven circulations, such as sea-, lake- and playa breezes, and slope- and valley wind circulations.

"Sagebrush"

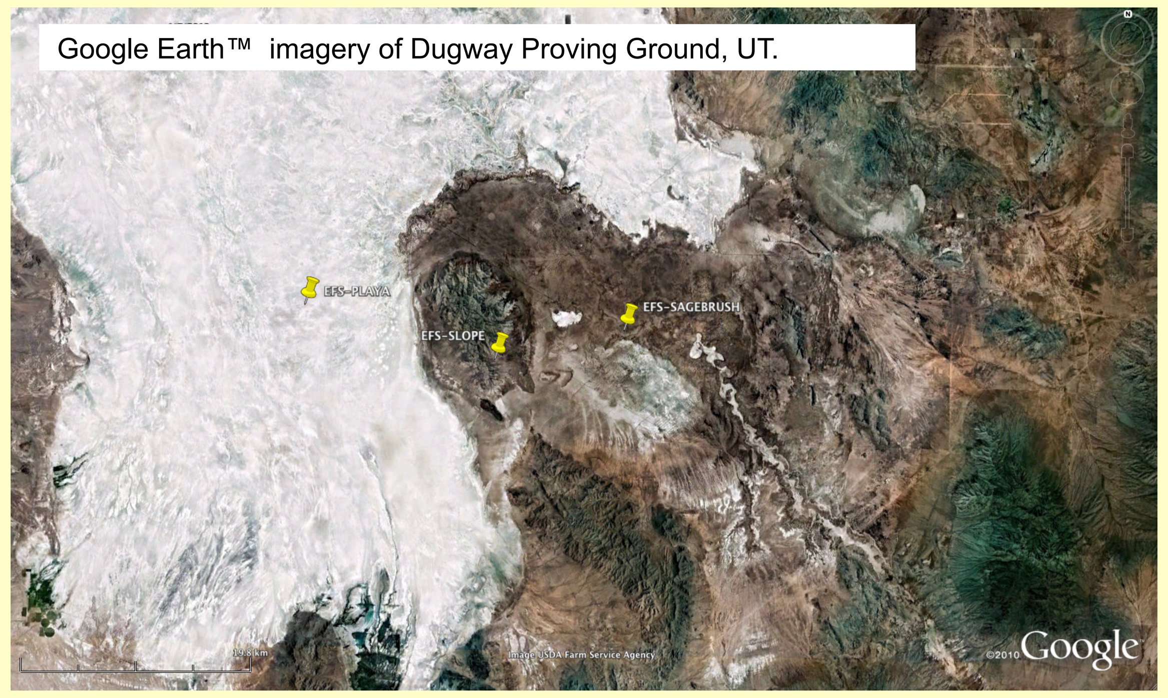


Google Earth™ imagery of Dugway Proving Ground, UT.

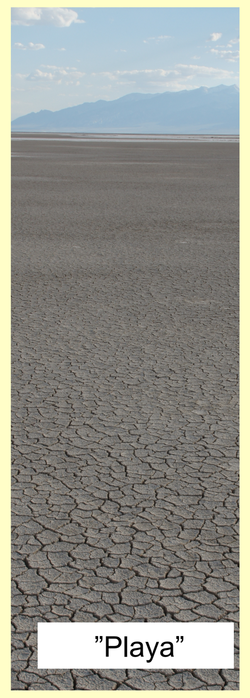

"Playa"

One objective of the experimental part of **MATERHORN** (Mountain Terrain Modeling and Observation Program) was to determine the local surface energy balance differences that would drive the circulation patterns under synoptically quiescent conditions. Three representative sites at Dugway Proving Ground were selected: one site (EFS-Sagebrush) is located in a large sparsely vegetated arid basin, a second (EFS-Playa) on a playa (dry alkali flats which fill with water seasonally to form shallow lakes), and a third (EFS-Slope) on the sparsely vegetated slope of an alluvial fan of Granite Peak.

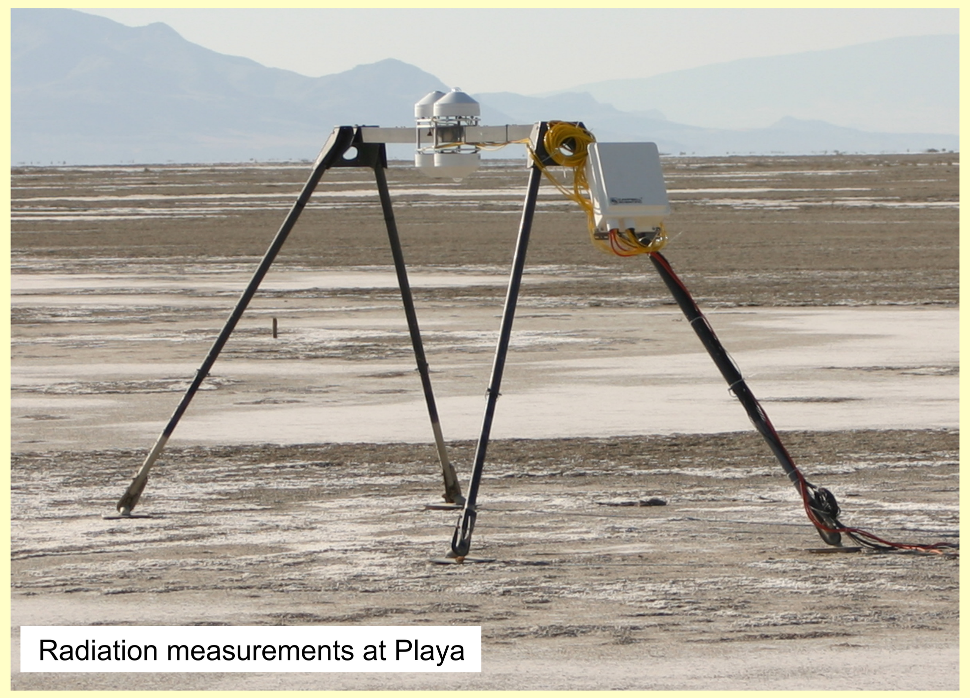

Radiation measurements at Playa

Tower at Playa

EC150 at Playa

## (2) SURFACE RADIATION AND ENERGY BALANCE DATA

All components of the surface energy balance (net radiation NR, sensible heat flux H, latent heat flux L and ground heat flux G) were directly measured at the three sites using some of the best available instrumentation. Besides the measurements of the individual short- and longwave components of the radiation balance and eddy-covariance measurements of the turbulent fluxes, our special focus was directed at the soil heat flux. Pairs of self-calibrating heat flux plates were used at all sites, and the heat storage term above the flux plates was calculated from soil temperature measurements at three levels along with direct observations of the soil's volumetric heat capacity.

## (3) RESULTS

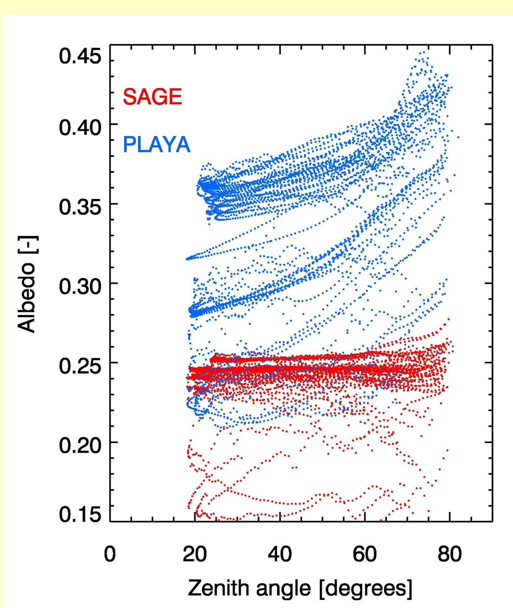


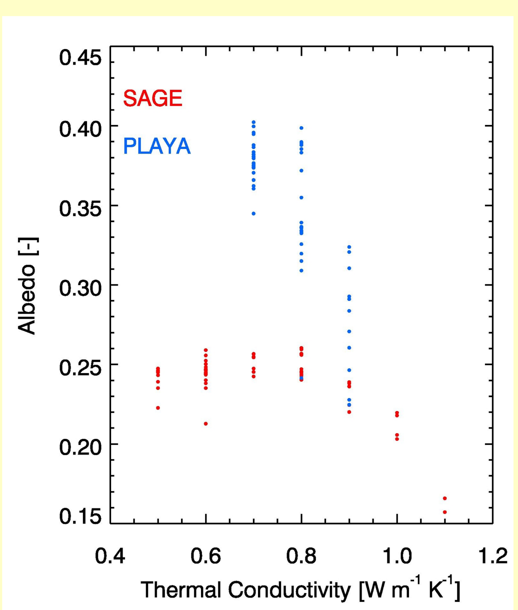


### a) Albedo

differences between the Playa and Sagebrush sites highlight the role of specular reflection. Soil moisture observations failed due to highly saline soils, but thermal conductivity variations indicate soil moisture effects on albedo.

TP01 thermal property sensor

### b) Radiation & energy balance components

for the Sagebrush and Playa sites on selected days during the MATERHORN FALL and SPRING campaigns: Measurements (solid lines) are compared to WRF simulations (symbols).

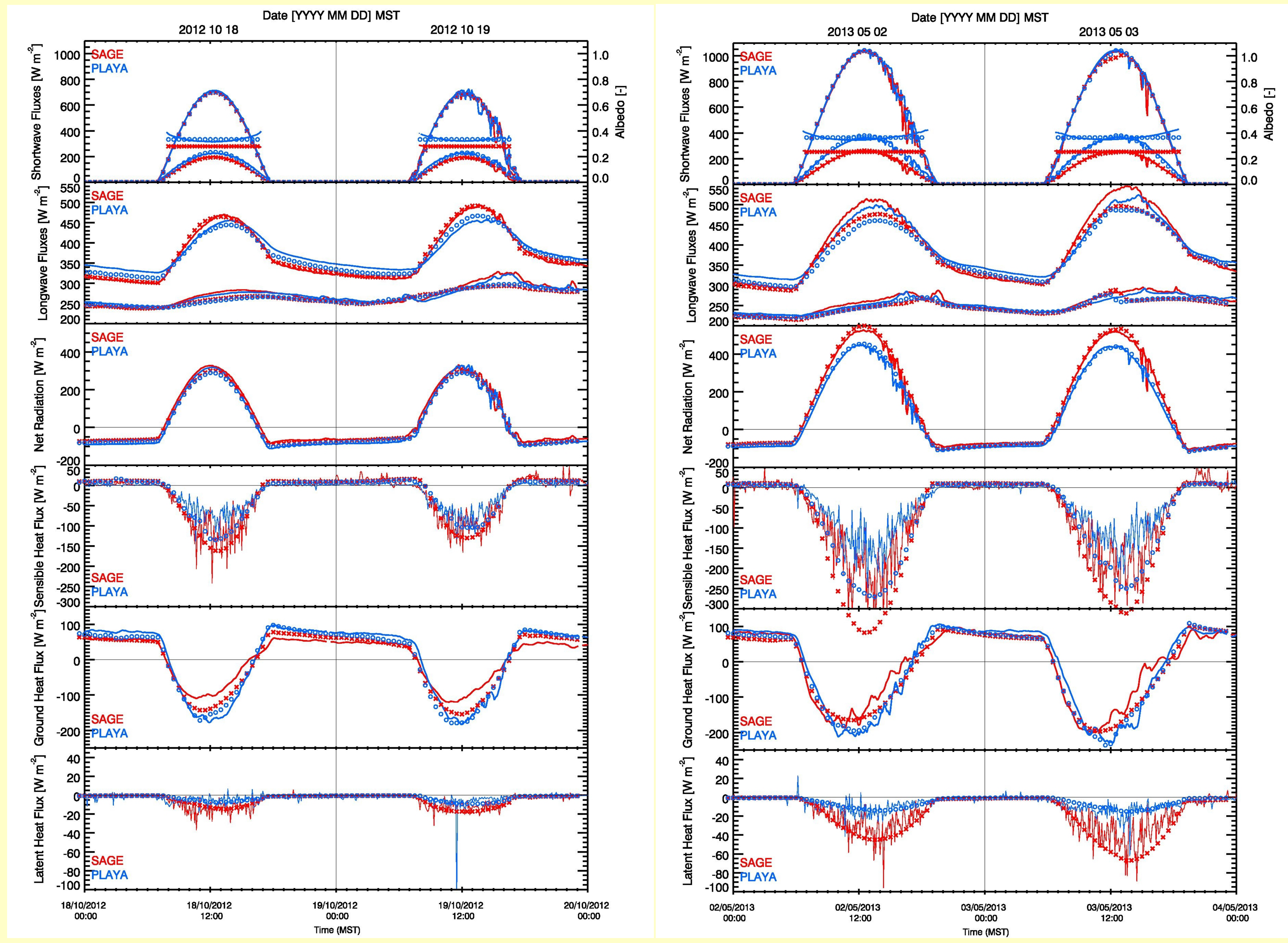


### c) Budget residual

While the energy balance is closed at nighttime, a large residual term is found during the day. Residuals of similar magnitude have been observed in many field campaigns. The cause for these residuals is still unknown. Comparisons with the WRF simulation points to an underestimation of the sensible heat flux.

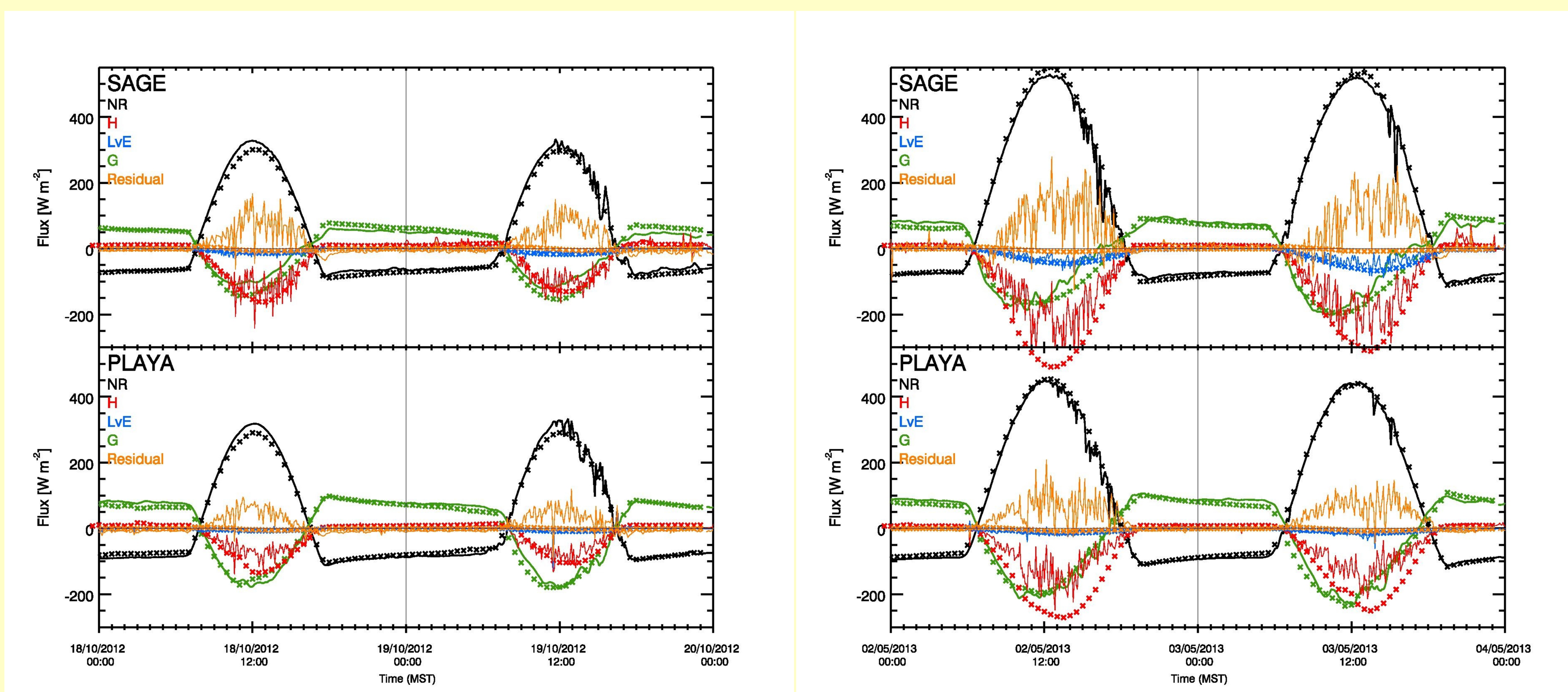


### d) Surface layer development

What is the response of these energy balance differences on the evolution of thermal structure of the atmosphere?

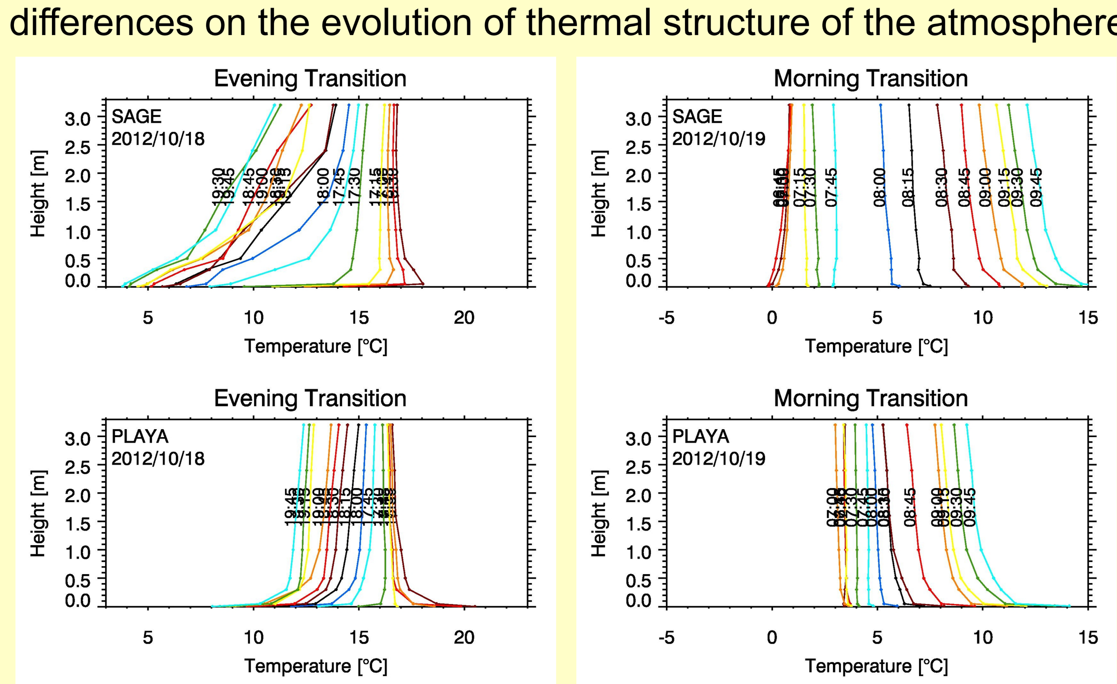


The Playa soil with its higher thermal conductivity takes up and releases more energy then the soil at the Sagebrush site. The release of this stored heat at Playa leads to a less rapid cooling of the near-surface air in the evening. In the morning, the heat uptake leads to less rapid near-surface heating.

### e) Boundary layer development

The difference in the energy balance affects the evolution of the entire boundary layer, as seen in tethersonde data.

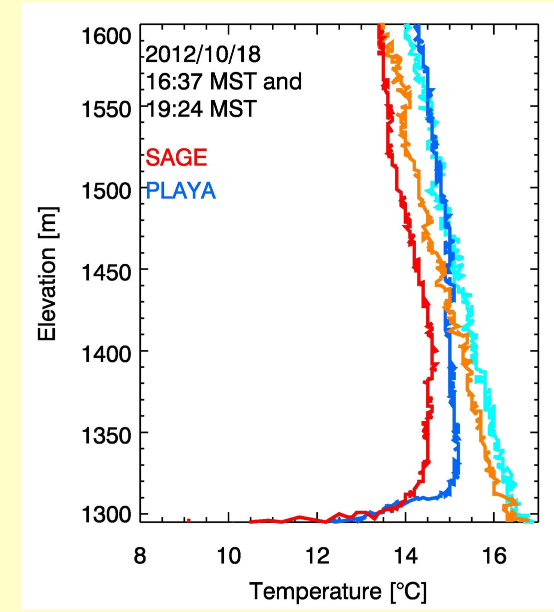


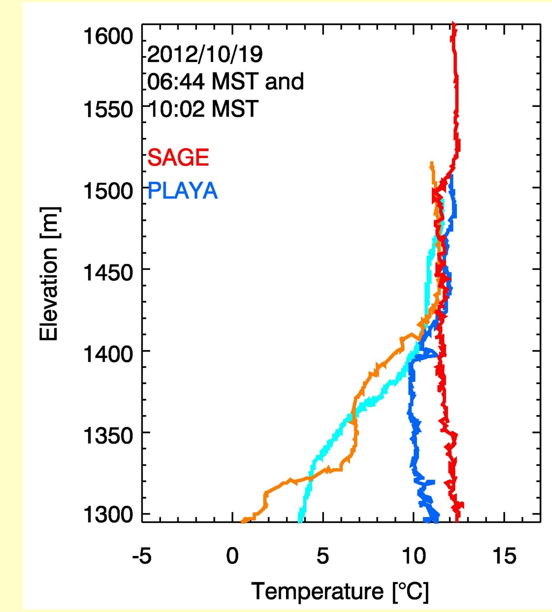


**WRF runs:** 3 km horizontal grid, initialized with 12 km NAM. 6 hour spin-up, Noah LSM, RRTMG radiation, ACM2 PBL parameterization, Thompson microphysics, no cumulus parameterization.
Observed albedo and soil moisture are prescribed. The thermal conductivity parameterization for silt loam as described by Massey et al. (2014) is used.

## (4) SUMMARY

**Radiation Balance:**

- Albedo differences among the sites are the main cause of variations in shortwave energy input. Differences are more pronounced in spring, as albedo values are then lower at Sagebrush and higher at Playa than in the fall.
- In the fall, the (smaller) effect of the albedo differences is compensated by higher longwave emission at Sagebrush, and net radiation differences are higher at night than during the day. In spring, daytime net radiation at Sagebrush exceeds values observed at Playa.
- Specular reflectance plays a role at Playa and leads to a pronounced diurnal cycle of albedo.
- Albedo at Playa varies with thermal conductivity (proxy for soil moisture).

**Ground Heat Flux:**

- The ground heat flux (G) plays an important role in the surface energy budget, especially at Playa, where thermal conductivities are high.
- During the night, the ground heat flux balances the net longwave loss.

**Turbulent Fluxes:**

- Latent heat fluxes (L) are very small at both sites. This is somewhat surprising given the shallow water table at Playa.
- During daytime, net radiation gets partitioned differently at the two sites. The greater ground heat flux at Playa reduces the amount of heat that is partitioned into sensible heat flux (H). Sensible heat flux dominates over ground heat flux at Sagebrush.
- During nighttime when H and L are near zero, the larger ground heat flux at Playa (as compared to Sagebrush) is compensated by the larger LW loss.

**Residual:**

- The energy balance is closed at night.
- A significant residual term remains during daytime when observation do not close the energy balance. WRF simulations show a higher sensible heat flux than observations, closing the balance.

Surface characteristics at the two study sites.

| Site | Sagebrush | | Playa | |
|---|---|---|---|---|
| Season | Fall | Spring | Fall | Spring |
| Albedo [-] | 0.27 | 0.24 | 0.31 | 0.33 |
| Thermal Conductivity [W m$^{-1}$ K$^{-1}$] | 0.59 | 0.73 | 0.98 | 0.79 |
| Roughness, $z_0$ [m] | 0.24 | | $6 \times 10^{-4}$ | |

## (5) ACKNOWLEDGMENTS

Funding comes from the Office of Naval Research Award N00014-11-1-0709. We thank all MATERHORN participants and DPG personnel involved in the project.